LAWRENCE
LIVERMORE
NATIONAL
LABORATORY

LLNL-JRNL-665284

Prebiotic hydrocarbon synthesis in impacting reduced astrophysical icy mixtures

L. Koziol, N. Goldman

December 10, 2014

The Astrophysical Journal

Disclaimer

This document was prepared as an account of work sponsored by an agency of the United States government. Neither the United States government nor Lawrence Livermore National Security, LLC, nor any of their employees makes any warranty, expressed or implied, or assumes any legal liability or responsibility for the accuracy, completeness, or usefulness of any information, apparatus, product, or process disclosed, or represents that its use would not infringe privately owned rights. Reference herein to any specific commercial product, process, or service by trade name, trademark, manufacturer, or otherwise does not necessarily constitute or imply its endorsement, recommendation, or favoring by the United States government or Lawrence Livermore National Security, LLC. The views and opinions of authors expressed herein do not necessarily state or reflect those of the United States government or Lawrence Livermore National Security, LLC, and shall not be used for advertising or product endorsement purposes.

Prebiotic hydrocarbon synthesis in impacting reduced astrophysical icy mixtures

Lucas Koziol and Nir Goldman

Physical and Life Sciences Directorate, Lawrence Livermore National Laboratory, Livermore, CA 94550

koziol@alumni.usc.edu, ngoldman@llnl.gov

Received _____; **accepted** _____

ABSTRACT

We present results of prebiotic organic synthesis in shock compressed reducing mixtures of simple ices from quantum molecular dynamics simulations extended to close to chemical equilibrium time-scales. Given the relative abundance of carbon in reduced forms in astrophysical ices as well as the tendency of these mixtures to form complex hydrocarbons under the presence external stimuli, it is possible that cometary impact could have yielded a larger array of prebiotic organic compounds than previously investigated. We find that the high pressures and temperatures due to supersonic compression yield a large assortment of carbon and nitrogen bonded extended structures that are highly reactive and have picosecond lifetimes. Expansion and cooling causes these materials to break apart and form a wide variety of potentially life-building compounds, including long-chain linear and branched hydrocarbons, large heterocyclic compounds, a variety of different amines, and exotic amino acids. Our results help provide a bottom-up understanding for hydrocarbon impact synthesis on early Earth and its role in producing life building molecules from simple starting materials.

Keywords: Origins of life, prebiotic chemistry, shock compression, comet impact, extreme thermodynamic conditions

1. Introduction

The origins of simple prebiotic hydrocarbons on early Earth such as amino acids and precursors to DNA and RNA has been debated without resolution since the seminal Miller-Urey experiments from over 60 years ago (Miller 1953; Miller & Urey 1959). These studies showed that electric discharges in a model early terrestrial system of methane, water, ammonia and hydrogen led to milligram quantities of amino acids including glycine, alanine, and α-amino-N-butyric acid. Reducing mixtures subjected to UV radiation (Sagan & Khare 1971; Bernstein et al. 2002), shock compression (Bar-Nun et al. 1970; McKay & Borucki 1997), and geothermal conditions (Harada & Fox 1964; LaRowe & Regnier 2008)

have produced prebiotic organic material such as amino acids and precursors to DNA and RNA nucleobases. However, the current viewpoint is that the composition of early Earth's atmosphere was more oxidizing (Brack 2007), consisting mainly of CO_2, with significantly lesser amounts of N_2, H_2S, HCl, and water vapor (Engel 2011). Shock heating experiments (Bar-Nun et al. 1970; McKay & Borucki 1997) and calculations (B. Fegley et al. 1986) on aqueous mixtures have found that synthesis of organic molecules necessary for amino acid production is less likely in a CO_2-rich environment.

The possibility exists that both prebiotic raw materials and energy may have been delivered to the Earth simultaneously by a cometary impact (Oro 1961; Chyba et al. 1990). Comets and astrophysical icy materials are heterogeneous materials predominantly composed of water, with significant concentrations of numerous other small molecules, including both oxidized and reduced forms of carbon (Ehrenfreund et al. 2002; Mumma & Charnley 2011). These compounds can comprise as much as 22% by concentration (Fomenkova et al. 1994; Herd et al. 2011) and include simple alkanes like methane (CH_4) and ethane (C_2H_6), small chain alcohols like methanol (CH_3OH), and nitriles such as HCN. Many of these compounds can act as precursors to prebiotic materials, and an impact can provide an abundant supply of energy to drive chemical reactivity. This could allow for prebiotic synthesis on a planet regardless of external constraints such as the presence of a catalyst, illuminating UV radiation, or other pre-existing conditions. Recent analysis of dust samples from comet Wild 2 have observed the presence of glycine in the captured material (Elsila et al. 2009). Interplanetary dust particles can accrete icy layers which can form animo acids upon exposure to UV radiation (noz Caro et al. 2002). The flux of organic matter to Earth via comets and asteroids during periods of heavy bombardment may have been as high as 10^{13} kg/yr, delivering up to several orders of magnitude greater mass of organics than what likely pre-existed on the planet (Blank et al. 2001).

Impacts on planetary surfaces can be divided into three distinct thermodynamic regions: (I) shock compression due to impact with the planet, (II) adiabatic (free) expansion due to the rarefaction wave passing through the icy material, and (III) cooling and equilibration due to heat transfer to materials extant on the planet. Given its relatively large size (e.g., median nucleus radius between 1.61 and 56 km (Meech et al. 2004)), a comet passing through

Earth's atmosphere will be heated externally but will remain cool internally. Upon impact with the Earth's surface, the resulting shock wave (Region I) will compress a small section of material on a time-scale that is limited by the rise time of the shock wave (< 10 ps) (Robertson et al. 1991; Gahagan et al. 2000; Kadau et al. 2002). A shock wave causes a reactive material to visit numerous thermodynamic states during the course of compression. Shock waves can create sudden, intense pressures and temperatures which could affect product branching pathways and reactions within a comet before interactions with the ambient planetary atmosphere can occur. An oblique collision where an extraterrestrial icy body impacts a planetary atmosphere with a glancing blow could generate thermodynamic conditions conducive to organic synthesis (Blank et al. 2001). Reactive conditions likely persist after arrival of the expansion wave (Region II) due to the remaining high temperature state, before cooling occurs (Region III) (Ross 2006). The cycling through of all three thermodynamic regions has been shown to yield significant concentrations of organic species in these systems (Goldman et al. 2010; Goldman & Tamblyn 2013). Shock compression experiments have shown that a high percentage of aqueous amino acids survived relatively low pressure conditions (412-870 K and 5-21 GPa; 1 GPa = 10 kbar) (Blank et al. 2001) and that mixtures resembling carbonaceous chondrites can produce a variety of organic material at pressures of $\sim$6 GPa (Furukawa et al. 2009). Nonetheless, to date there have been few studies on the production of prebiotic molecules at both extreme temperatures and pressures (e.g., $>$1000 K and 20 GPa) that can result from oblique impact of a large icy body such as a comet.

Molecular dynamics (MD) simulations can provide an accurate description of the chemical reactivity with a shock compressed body (Goldman et al. 2009a,b; Manaa et al. 2009; Ileri & Goldman 2014) which can greatly facilitate experimental design and interpretation. After impact, a comet of standard size would be held in a hot, compressed state on the order of seconds before arrival of a rarefaction wave and subsequent decompression. However, chemical kinetics are likely to achieve equilibrium over many orders of magnitude shorter time scales, e.g., nanoseconds (Manaa et al. 2009; Goldman & Bastea 2014). These timescales are amenable to high throughput simulation approaches(Goldman & Fried 2012; Goldman et al. 2013; Srinivasan et al. 2014; Goldman 2014) and could be probed directly by state of

the art laser shock-compression experiments (Armstrong et al. 2013). Our initial quantum simulations on a CO_2-rich aqueous mixture showed the possibility of formation of the proteinogenic amino acid glycine due to shock synthesis (Goldman et al. 2010), as well as possible precursors for nucleotides of DNA and RNA and many small prebiotic molecules (Goldman & Tamblyn 2013). Our results have since been confirmed by shock recovery experiments on a similar mixture, where several linear and methyl-amino acids including glycine have been produced (Martins et al. 2013). However, our simulations were limited to the oxidizing icy mixture alone, and experiments so far have been designed to detect synthesized amino acids therein, exclusively. Further experimentation would greatly benefit from detailed knowledge of the types of prebiotic molecules in addition to amino acids that can occur as a function of different chemical compositions of the initial icy mixture subjected to a variety of peak thermodynamic conditions.

Given the heterogeneity of a comet or astrophysical icy mixture, there exists a likelihood of regions existing within these materials that are rich in reduced forms of carbon (e.g., CH_4, HCN) that promote prebiotic synthesis more readily than the oxidizing mixture of our previous study. HCN in particular has been found in cometary ices in relatively high concentrations (Ehrenfreund & Charnley 2000), and has been detected throughout our galaxy, in interstellar clouds, cosmic dust, carbonaceous chondrites, and comets in detectable amountsSnyder & Buhl (2012); Matthews & Minard (2006); Ehrenfreund et al. (2002); He et al. (2012). Significant concentrations of HCN can be produced upon planetary impact (Goldman et al. 2010; Goldman & Tamblyn 2013). Liquid HCN is known to polymerize spontaneously in the presence of a base, such as an amine or ammonia, or in the presence of incident UV radiation (Matthews & Minard 2006), yielding products such as the nucleobase adenine and heteropolypeptides (protein forming chains of different amino acids). The actual involvement of all prebiotic extraterrestrial material in life-forming chemistry on Earth would be dictated in large part by their reactivity upon delivery to the planet. To the best of our knowledge, a detailed inventory of possible chemical products from shock synthesis within these types of mixtures has yet to be conducted.

To address these issues in detail, we have conducted quantum simulations of reduced prebiotic mixtures containing HCN to near chemical equilibrium timescales under the entire

impact cycle of heating and compression, followed by expansion and cooling. We find that shock compression yields high pressure and temperature states, which results in the partial condensation of carbon and nitrogen into larger, extremely short-lived particles with varying numbers of C-C and C-N bonds. Relaxation and cooling to low pressure and temperature states ultimately allows for the formation of a much richer variety of new, stable compounds than our previous studies, including some amino acids and their precursors, and several aromatic species. Knowledge of these properties will help create a chemical "road map" understanding for hydrocarbon impact synthesis on early Earth and its role in producing prebiotic molecules.

2. Computational details

DFTB calculations with self-consistent charges (SCC) (Elstner et al. 1998) were driven by the LAMMPS molecular software simulation suite (Plimpton 1995), with the DFTB+ code (Aradi et al. 2007) used to compute forces and the cell stress tensor. C-H-O-N interaction parameters were used that are available for download (mio-0-1 parameter set from http://www.dftb.org). For each MD time step, the maximum number of SCC steps was limited to four through use of the Extended Lagrangian Born-Oppenheimer MD (XL-BOMD) approach for propagation of the electronic degrees of freedom (Zheng et al. 2011). Thermal populations of the electrons were computed through the Mermin functional (Mermin 1965). All simulations discussed here were performed with a time-step of 0.2 fs. We used an initial astrophysical ice composition of 24 H_2O, 12 CH_4, 12 CH_3OH, 12 HCN, and 12 NH_3(288 atoms total), with periodic boundary conditions used to approximate a mesoscale system size. Initial computational cell lattice vectors were $a = 21.6983$ Å, and $b = c = 10.8492$ Å, corresponding to a density of 1.0 g/cc. This density is close to that of similar studies (Goldman et al. 2010; Goldman & Tamblyn 2013; Martins et al. 2013). Initial equilibration at 300K was performed for 10 ps using Nose-Hoover thermostat chains (Nosé 1984; Hoover 1985). Uniaxial compression due to the shock wave and adiabatic expansion of the rarefaction wave occurred along the a lattice vector. Previous work has shown that doubling the system size along the a lattice vector yielded virtually identical thermodynamic conditions under

shock loading (Goldman et al. 2010).

Shock compression simulations were conducted using the well-established Multi-scale Shock compression Simulation Technique (MSST) (Reed et al. 2003). MSST operates by time-evolving equations of motion for the atoms and the computational cell dimension in the direction of the shock to constrain the stress in the propagation direction to the Rayleigh line and the energy of the system to the Hugoniot energy condition. (The Hugoniot is the locus of thermodynamic end states achieved by a specific shock velocity and set of initial conditions.). For a given shock speed, these two relations describe a steady planar shock wave within continuum theory. MSST has been used in conjunction with quantum simulation methods to accurately reproduce the shock Hugoniot of a number of systems (Mundy et al. 2008; Goldman et al. 2009b, 2010; Goldman & Fried 2012; Goldman et al. 2013; Reed 2012). Quantum nuclear vibrational effects are known to result in higher Hugoniot temperatures (Goldman et al. 2009a) and enhanced chemical reactivity (Qi & Reed 2012) under extreme conditions compared to purely classical ionic trajectories. Here, we analyze results from classical MD trajectories only. For all shock velocities, we used a scaling term with the MSST ionic equations of motion to account for drift in the conserved quantity in our simulations (Srinivasan et al. 2014; Goldman & Bastea 2014). A scaling factor of 10^{-3} resulted in a deviation in the total forces in our simulations of less than 1% once a steady shock compression had been produced. We allowed the system to evolve for up to ∼150 ps within the shock state.

Adiabatic expansion simulations were conducted using the DOLLS algorithm (Hoover et al. 1980), where the simulation cell was expanded at a constant rate until the initial density of 1.0 g/cc was achieved. The DOLLS algorithm uses an alternate Hamiltonian to alter the simulation cell volume at a constant rate while ensuring that the system is constrained to visit the thermodynamic states corresponding to its adiabat, i.e., $dE_{tot} = -PdV$. In previous work the expansion rates were varied between 10 and 100 ps, and although these timescales are significantly shorter than those of experiments or an actual impact, it was found that chemical reactivity was consistent for values of $k_X^{-1} > 50$ps (Goldman & Tamblyn 2013; Ileri & Goldman 2014). In this work we used $k_X^{-1} = 60$ ps in all of our simulations. Following adiabatic expansion, the simulations were cooled from their high temperature state to 300

K over 30 ps using a temperature ramp, followed by a further equilibration step at 300 K for 30 ps using Nose-Hoover thermostat chains. Calculations corresponding to the longest expansion rate had a total simulation time (Regions I, II, and III) of approximately 260 ps, and encompassed a wide range of different thermodynamic conditions (2). The time frame on which a comet impact occurs is on the order of seconds (Goldman et al. 2010), which is well beyond the means of molecular dynamics simulations. However, our simulations reported here describe processes and dynamics on a timescale several orders of magnitude larger than the picosecond rise-time of shocks in polycrystalline materials (Robertson et al. 1991; Gahagan et al. 2000; Kadau et al. 2002; Armstrong et al. 2010; Crowhurst et al. 2011), shock compressed water (Goldman et al. 2009b), and our previous quantum simulations (Goldman et al. 2010). In addition, explosive disintegration of cosmic bodies can also occur upon entering the Earth's atmosphere (Fortov et al. 2013). The resulting ejecta can be composed of particles between 100 microns to 10 meters in diameter (Lorenz 2004), all of which will compress and subsequently expand and cool extremely rapidly. Our impact simulations thus span the relevant time scales corresponding to the chemistry within icy grains in a comet. Our simulation timescales are amenable to study by laser shock compression experiments (Gahagan et al. 2000; Armstrong et al. 2010; Crowhurst et al. 2011).

3. Results and discussion

Simulations were conducted for shock velocities of 7 – 12 km s^{-1}, which yielded Hugoniot pressures of 20 – 82 GPa and temperatures of 1000 – 3900 K (Fig. 1). The particle velocity U_P from our shock compression simulations was taken to be equal to the impact velocity Goldman et al. (2010), and is related to the angle from the horizon ϕ according to the formula: $U_P = (V_E/2)\sin\phi$. Here, U_P is computed according to the relation $U_P = U_S(1 - \rho_0/\rho)$, where U_S is the shock velocity imparted to the system and ρ_0 is the density of the initial pre-shock state, and V_E is the encounter velocity of the impacting extraterrestrial icy object. Impact with an ocean or other body with similar shock impedance to the extraterrestrial ice contributes an approximate factor of 1/2 due to the body's compressibility. An astrophysical ice with initial velocity of 29 km s^{-1} (approximate median encounter velocity of a short period

comet with Earth (Blank et al. 2001)) would have to impact the Earth at an angle from the horizontal of up to 28° to experience the pressures and temperatures of our simulations. Assuming a probability distribution of $dP = \sin(2\phi)d\phi$, where ϕ is the angle from the horizon (Shoemaker 1962), our simulations correspond to low velocity impacts with a cumulative 22% probability. Thus, our study encompasses likely events for astrophysical ice impacts on early Earth.

Our trajectories indicate rapid chemical reactivity in our simulations at Hugoniot conditions of 52 GPa and 2500 K, 67 GPa and 2300 K, and 82 GPa and 3900 K. Hence, we choose to focus our analysis on these trajectories. Analysis of configurations from our simulations indicates that the high pressure-temperature states due to shock compression result in the rapid decomposition of our starting materials (Fig. 2(a)). These in turn form new bonds, in particular between carbon and nitrogen bonds, which can form extended structures with multiple bonding arrangements. Time traces of the equation of state state during shock compression indicates that the system achieves a steady thermodynamic state in a few picoseconds, with the exception of the 52 GPa trajectory (Fig. 2(b)). Here, the system temperature is monotonically increasing, which is commensurate with chemical reactivity that is longer than the timescales of our simulations. Nanosecond chemical timescales have been observed in a a number of organic mixtures under shock loading due to slow carbon coagulation kinetics (Reed et al. 2008; Manaa et al. 2009). After concluding adiabatic expansion from the shock Hugoniot states, all of our simulations achieve low pressures and densities, but remain in relatively high temperature states, with the 52 GPa simulation at a temperature of 1500 K, the 67 GPa simulation a temperature of 1900 K, and the 82 GPa simulation a temperature of 2200 K. We observe a number of C-N bonded oligomers in this state, as well as some smaller C-C ands C-N bonded fragments. Upon cooling and equilibration to 300 K and 1 g/mL density we observe that all of these fragments and oligomers have coalesced into several different C-N bonded structures with different functional groups (e.g., C-OH, etc.).

Amino acids contain both amine (-NH_2) and carboxyl (-COOH) functional groups, and require carbon-nitrogen bond formation for their synthesis. Protein synthesis is driven by peptide bond formation, i. e., C–N bonds formed between -COOH and -NH_2 groups from

different amino acids while eliminating an H_2O molecule. Larger life-building compounds such as many protein forming acids and nucleotides of RNA and DNA require the formation of extended carbon bonded networks (Goldman & Tamblyn 2013; Ehrenfreund et al. 2006). Hence, our goal is to create a more fundamental understanding of C-C and C-N bond formation as a function of elevated temperature and pressure due to shock compression. Analysis of the radial distribution functions (RDFs) for each type of bonding pair can provide a general picture for the different types of bonds that form during impact events, viz., $g(R) = V/N^2 \left\langle \sum_{i<j} \delta(r - r_{ij}) \right\rangle$. Here, V is the volume of our simulation cell, N is the number of particles in the system, and r_{ij} is the distance between a given $i-j$ bonded pair. For shock conditions of 52 GPa, we observe that the peak at 1.1 Å corresponding to the C-N triple bond in HCN disappears after several picoseconds due to its decomposition. Consequently, we observe the simultaneous formation of reduced forms of carbon and nitrogen bonded compounds such as amines (e.g. R-CH_2-NH_2, where R is an unspecified group or molecule and the C-N bond is single), with a peak in the RDF at ∼1.4 Å, although the peak is quite broad and could contain many different forms of C-N bonded compounds. Concurrently, we observe the formation of new C-C bonds after several picoseconds, centered around 1.5 Å consistent with graphite and diamond nearest neighbor distances of ∼1.42 and 1.55 Å, respectivelyGoldman & Fried (2012); Goldman et al. (2013). During adiabatic expansion, the C-C bond peak has shifted to slightly higher distance due to the lower pressures attained. Upon cooling and equilibrating, we observe the formation of three distinct C-N bonded peaks: one at ∼1.1 Å likely corresponding to nitrile groups (e.g., R-CN, where carbon and nitrogen have a triple bond), one at ∼1.3 Å possibly corresponding to imine groups (e.g., C-N double bond), and one at ∼1.4 Å likely corresponding to amine groups. We also observe C-C bonded peaks at distances of 1.4 Å and 1.55 Å consistent with the formation of sp^2 and sp^3-bonded carbon structures.

We now determine the specific chemical reactivity and bond kinetics in our shock compression simulations (Region I) using a pre-established methodology of optimal bond cutoff distances and lifetimes (Goldman et al. 2005; Goldman & Fried 2006, 2007; Goldman et al. 2010). We observe that the sudden increase in pressure and temperature due to shock loading causes the starting materials to become highly reactive, with many compounds

having computed lifetimes of hundreds of femtoseconds or less. Given the short chemical lifetimes and complex reactivity in our simulations, we have generalized chemical events by examining the time traces of concentrations of total C-C and C-N bonds (Fig. 4). This allows for a detailed chemical picture under these conditions without relying on the fate of specific compounds and any intermediates they might form. At shock conditions of 52 GPa, we observed that C-C bond formation is increasing monotonically, and has not yet achieved a steady kinetic state on the timescales of our simulations, e.g., there is persistent growth of carbon containing clusters. In contrast, the 67 GPa trajectory is considerably closer to equilibrium in terms of C-C bond formation. These conditionsyield the highest concentration of C-C bonds, which could indicate that the higher degree of complexity in terms of organic products could be achieved under these conditions. The 82 GPa trajectory achieves C-C bond formation steady state within the first 20 ps off the simulation, largely due to the intense pressurization and thermalization under these shock conditions. In terms of C-N bond formation, the initial value for the its concentration for each simulation is due to the presence of HCN as a starting material. At 52 GPa we observe that a steady state appears to have formed over the timescale of our simulation, indicating that under these conditions C-N bond forming kinetics occur more rapidly than those for C-C bonds. In contrast, the 67 GPa and 82 GPa simulations show that the number of C-N bonds in at these conditions decreases overall, indicating that C-C bonding is favored in the clusters formed under these conditions.

Our molecular analysis shows that the reactive shock conditions studied here yield a large number of specific C-C and C-N bonded oligomers (molecular complexes), with lifetimes generally less than 0.05 ps. However, these oligomers tend to be composed of a series of longer-lived C-C and C-N bonded backbones, with smaller moieties such as hydroxyl groups diffusing on and off the backbones at rapid rates. We note that in general the C-C and C-N bonded backbones that can form are significantly larger and more complex than those observed in our impact simulations of an icy mixture under oxidizing conditions (Goldman & Tamblyn 2013). At shock pressures of 52 GPa, we observe a wide variety of C-C and C-N bonded complexes (Fig. 5), with small clusters containing only 1-2 bonds of each type having lifetimes on the order of 5 ps, and larger oligomers with as many as 14 C-C bonds and 17 C-N bonds with lifetimes of several hundred femtoseconds. Shock pressures of 67

GPa have produced the richest array of C-C and C-N bonded oligomers of the three sets of conditions studied here, though the lifetimes of smaller clusters is reduced to approximately 1 ps. In general, C-C and C-N bonded oligomers under these conditions tended to contain larger numbers of C-C bonds, with backbones containing as many as 29 C-C bonds and 15 C-N bonds. The lifetimes of these species were again computed to be on the order of several hundred femtoseconds. The C-C and C-N backbones formed under shock conditions of 82 GPa tended to be smaller overall and with shorter lifetimes, with all clusters exhibiting computed lifetimes of less than 1 ps due to the higher thermodynamic conditions.

Relaxation to low density and low temperature conditions (Regions II and III) caused the large C-C and C-N bonded oligomers due to break apart into smaller fragments and form a series of new, stable compounds (Fig. 6). All of our simulations recovered significant amount of water, as well as NH_3, and HCN. Expansions from 52 GPa and 67 GPa yielded significant amounts of CH_4, and expansion from 82 GPa yielded both ethane (CH_3CH_3, 30 atomic mass units or amu) and propene (CH_3CHCH_2, 42 amu). Aqueous mixtures of simple hydrocarbons with NH_3have been shown to yield protein forming amino acids under shock compression (Bar-Nun et al. 1970) and ultraviolet irradiation (Sagan & Khare 1971). Expansions from peak conditions of 52 GPa produced a number of aliphatic amines, e.g., an NH_2 containing compound with no aromatic rings attached directly to the nitrogen. We observe the formation of methylamine (CH_3NH_2, 31 amu) and propylamine $CH_3CH_2CH_2NH_2$, 59 amu). Small chain amines have been observed in recovered cometary materials (Glavin et al. 2008) and meteorites (Aponte et al. 2014), and have been proposed as significant constituents of Titan's atmosphere (Cable et al. 2014). These types of amines share structural features with amino acids such as carbon backbones and chiral centers, and could serve as possible precursors to amino acid synthesis in astrophysical bodies via a Strecker-type synthesis (Aponte et al. 2014). We note the formation of an amine compound at 99 amu containing two imine groups (C-N double bonds), which could serve as a precursor to peptide chain of amino acids with multiple chiral centers. We also observe ethanolamine (61 amu), and which has been observed in collected cometary dust (Glavin et al. 2008), is both commonly found as a biological membrane precursor and as a component of some neurotransmitters (Calignano et al. 2001). The largest molecule produced from these conditions (294 amu) is a complex amino acid

that contains a moiety chemically similar to glycine as well as three adjoined aromatic rings, i.e., two six-membered rings of the form C_5N and one five-membered ring containing carbon, only (shown in detail in Fig. 7(a)). This structure indicates the possibility of shock synthesis of protein building heteropolypeptides without the intervening formation of α-amino acids, similar to previous studies under ambient conditions (Matthews 1991). In addition, polycyclic aromatic hydrocarbons have been proposed as possible precursors to nucleotides of DNA and RNA (Ehrenfreund et al. 2006).

Expansion from 67 GPa yielded a somewhat similar array of small chain C-N bonded compounds, including methylamine and propynylamine (55 amu). We also observe proprionitrile and methylehtylene alcohol at the same molecular mass. These conditions also yielded a long chain imine compound containing nine carbon atoms (151 amu), and an alcohol comound containing an aromatic imideazole ring (138 amu; shown in detail in Fig. 7(b)), which is somewhat similar chemically to the protein forming amino acids histidine. Expansion from 82 GPa yielded the hydrocarbons ethane and propene (42 amu), as well as formaldehyde (30 amu) and ketene (42 amu). Formaldehyde can react with cyano groups and NH_3 to form amino acids via Strecker synthesisBrack (2007). Ketene is a highly reactive compound that has been observed in the interstellar medium (Maity et al. 2014). These conditions also yielded a long-chain amine compound (200 amu), containing 14 carbon atoms with multiple double and one triple C-C bond. Long-carbon chain compounds are essential components of phospholipids found in biological membranes as well as fatty acids commonly found in biological materials, and smaller functionalized long-chain molecules could contribute to the vesicle stability of these materials (Rendón et al. 2012).

4. Conclusions

Our results yield insight into the shock synthesis of both simple and complex hydrocarbons from impacting reducing icy mixtures and pertain to the chemistry of prebiotic compounds produced in space that could be delivered to a planet. All of the reactive conditions studied here yielded a wide variety of amines and other carbon and nitrogen bonded compounds that are likely precursors to terrestrial amino acids. Simulated impacts

corresponding to peak thermodynamic conditions of 52 GPa and 2500 K yielded a large amino acid with nitrogen-containing polycyclic aromatic rings and a segment corresponding to the amino acid glycine. This indicates that peptides and other complex biological molecules could be produced within astrophysical ices during impact events. Peak conditions of 67 GPa and 3200 K yielded an imideazole containing compound that could indicate a synthetic route for the protein forming amino acid histidine. Finally, the strongest shock conditions studied here of 82 GPa and 3900 K yielded an unsaturated long-chain amine compound, with multiple types of C-C bonds. More direct impacts with early Earth such as those studied here could have yielded a variety of theses types of molecules that could have eventually been incorporated into biological membranes, fatty acids, or other materials essential for life. This is in contrast to our previous studies of shock synthesis in oxidizing icy mixtures, which tended to yield a more limited array of prebiotic hydrocarbons under somewhat less intense thermodynamic conditions (e.g., less probable impacts). Our results provide a mechanism for the shock synthesis of prebiotic materials on extra-terrestrial environments as well, such as within the dense hydrocarbon atmosphere of Titan (Raulin et al. 2012; Kaiser & Mebel 2012) or within the icy, hydrocarbon containing crust of Enceladus (Martins et al. 2013). This helps to create a simple chemical picture for the chemistry of these prebiotic molecules during well known periods of heavy comet and asteroid bombardment that is independent of external features such as the presence of a catalyst, illuminating UV radiation, or pre-existing conditions on a planet.

5. Acknowledgments

This work was performed under the auspices of the U.S. Department of Energy by Lawrence Livermore National Laboratory under Contract DE-AC52-07NA27344, and was funded by the National Aeronautics and Space Administration (NASA), under the Astrobiology: Exobiology and Evolutionary Biology program (#NNH11AQ67I). Computations were performed at LLNL using the Aztec and RZCereal massively parallel computers.

REFERENCES

Aponte, J. C., Dworkin, J. P., & Elsila, J. E. 2014, Geochimica et Cosmochimica Acta, 141, 331

Aradi, B., Hourahine, B., & Frauenheim, T. 2007, J. Phys. Chem. A, 111, 5678, http://www.dftb-plus.info

Armstrong, M. R., Crowhurst, J. C., Bastea, S., & Zaug, J. M. 2010, Journal of Applied Physics, 108, 023511

Armstrong, M. R., Zaug, J. M., Goldman, N., Kuo, I.-F. W., Crowhurst, J. C., Howard, W. M., Carter, J. A., Kashgarian, M., Chesser, J. M., Barbee, T. W., & Bastea, S. 2013, J. Phys. Chem. A, 117, 13051

B. Fegley, J., Prinn, R. G., Hartman, H., & Watkins, G. H. 1986, Nature, 319, 305

Bar-Nun, A., Bar-Nun, N., Bauer, S. H., & Sagan, C. 1970, Science, 168, 470

Bernstein, M. P., Dworkin, J. P., Sandford, S. A., Cooper, G. W., & Allamandola, L. J. 2002, Nature, 416, 401

Blank, J. G., Miller, G. H., Ahrens, M. J., & Winans, R. E. 2001, Origins Life Evol. B, 31, 15

Brack, A. 2007, Chemistry and Biodiversity, 4, 665

Cable, M. L., Hörst, S. M., He, C., Stockton, A. M., Mora, M. F., Tolbert, M. A., Smith, M. A., & Willis, P. A. 2014, Earth and Planetary Science Letters, 403, 99

Calignano, A., Rana, G. L., & Piomelli, D. 2001, European Journal of Pharmacology, 419, 191

Chyba, C. F., Thomas, P. J., Brookshaw, L., & Sagan, C. 1990, Science, 249, 366

Crowhurst, J. C., Armstrong, M. R., Knight, K. B., Zaug, J. M., & Behymer, E. M. 2011, Phys. Rev. Lett., 107, 144302

Ehrenfreund, P. & Charnley, S. B. 2000, Annu. Rev. Astron. Astrophys, 38, 427

Ehrenfreund, P., Irvine, W., Becker, L., Blank, J., Brucato, J. R., Colangeli, L., Derenne, S., Despois, D., Dutrey, A., Fraaije, H., Lazcano, A., Owen, T., Robert, F., & an International Space Science Institute ISSI-Team. 2002, Rep. Prog. Phys., 65, 1427

Ehrenfreund, P., Rasmussen, S., Cleaves, J., & Chen, L. 2006, Astrobiology, 6, 490

Elsila, J. E., Glavin, D. P., & Dworkin, J. P. 2009, Meteorit. Planet. Sci., 44, 1323

Elstner, M., Porezag, D., Jungnickel, G., Elsner, J., Haugk, M., Frauenheim, T., Suhai, S., & Seifert, G. 1998, Phys. Rev. B, 58, 7260

Engel, M. H. 2011, in Proceedings of SPIE, Vol. 8152, Instruments, Methods, and Missions for Astrobiology XIV, ed. R. Hoover, P. Davies, G. Levin, & A. Rozanov, SPIE (1000 20th St., PO Box 10, Bellingham, WA 98227-0010 USA: SPIE-Int Soc Optical Engineering), conference on Instruments, Methods, and Missions for Astrobiology XIV, San Diego, CA, AUG 23-25, 2011

Fomenkova, M. N., Chang, S., & Mukhin, L. M. 1994, Geochim. Cosmochim. Acta, 58, 4503

Fortov, V. E., Sultanov, V. G., & Shutov, A. V. 2013, Geochemistry International, 51, 549

Furukawa, Y., Sekine, T., Oba, M., Kakegawa, T., & Nakazawa, H. 2009, Nat. Geosci., 2, 62

Gahagan, K. T., Moore, D. S., Funk, D. J., Rabie, R. L., & Buelow, S. J. 2000, Phys. Rev. Lett., 85, 3205

Glavin, D. P., Dworkin, J. P., & Sandford, S. A. 2008, Meteoritics & Planetary Science, 43, 399

Goldman, N. 2014, Chem. Phys. Lett., http://dx.doi.org/10.1016/j.cplett.2014.11.037

Goldman, N. & Bastea, S. 2014, J. Phys. Chem. A, 118, 2897

Goldman, N. & Fried, L. E. 2006, J. Chem. Phys., 125, 044501

—. 2007, J. Chem. Phys., 126, 134505

—. 2012, J. Phys. Chem. C, 116, 2198

Goldman, N., Fried, L. E., Kuo, I.-F. W., & Mundy, C. J. 2005, Phys. Rev. Lett., 94, 217801

Goldman, N., Reed, E. J., & Fried, L. E. 2009a, J. Chem. Phys., 131, 204103

Goldman, N., Reed, E. J., Fried, L. E., Kuo, I.-F. W., & Maiti, A. 2010, Nat. Chem., 2, 949

Goldman, N., Reed, E. J., Kuo, I.-F. W., Fried, L. E., Mundy, C. J., & Curioni, A. 2009b, J. Chem. Phys., 130, 124517

Goldman, N., Srinivasan, S. G., Hamel, S., Fried, L. E., Gaus, M., & Elstner, M. 2013, J. Phys. Chem. C, 117, 7885 , http://dx.doi.org/10.1021/jp312759j

Goldman, N. & Tamblyn, I. 2013, The Journal of Physical Chemistry A, 117, 5124

Harada, K. & Fox, S. 1964, Nature, 201, 335

He, C., Lin, G., Upton, K. T., Imanaka, H., & Smith, M. A. 2012, The Journal of Physical Chemistry A, 116, 4751

Herd, C. D. K., Blinova, A., Simkus, D. N., Huang, Y., Tarozo, R., Alexander, C. M. O. D., Gyngard, F., Nittler, L. R., Cody, G. D., Fogel, M. L., Kebukawa, Y., Kilcoyne, A. L. D., Hilts, R. W., Slater, G. F., Glavin, D. P., Dworkin, J. P., Callahan, M. P., Elsila, J. E., Gregorio, B. T. D., & Stroud, R. M. 2011, Science, 332, 1304

Hoover, W. G. 1985, Phys. Rev. A, 31, 1695

Hoover, W. G., Evans, D. J., Hickman, R. B., Ladd, A. J. C., Ashurst, W. T., & Moran, B. 1980, Phys. Rev. A, 22, 1690

Ileri, N. & Goldman, N. 2014, J. Chem. Phys, 141, 164709

Kadau, K., Germann, T. C., Lomdhal, P. S., & Holian, B. L. 2002, Science, 296, 1681

Kaiser, R. I. & Mebel, A. M. 2012, Chem. Soc. Rev., 41, 5490

LaRowe, D. & Regnier, P. 2008, Origins of Life and Evolution of the Biosphere, 38, 383

Lorenz, R. D. 2004, Meteorit. Planet. Sci., 39, 617

Maity, S., Kaiser, R. I., & Jones, B. M. 2014, Astrophys. J., 789, 36

Manaa, M. R., Reed, E. J., Fried, L. E., & Goldman, N. 2009, J. Am. Chem. Soc., 131, 5493

Martins, Z., Price, M. C., Goldman, N., Sephton, M. A., & Burchell, M. J. 2013, Nat. Geosci., 6, 1045

Matthews, C. N. 1991, Origins of life and evolution of the biosphere, 21, 421

Matthews, C. N. & Minard, R. D. 2006, Faraday Discuss., 133, 393

McKay, C. P. & Borucki, W. J. 1997, Science, 276, 390

Meech, K. J., Hainaut, O. R., & Marsdenc, B. G. 2004, Icarus, 170, 463

Mermin, N. D. 1965, Phys. Rev., 137, 1441

Miller, S. L. 1953, Science, 117, 528

Miller, S. L. & Urey, H. C. 1959, Science, 130, 245

Mumma, M. J. & Charnley, S. B. 2011, Annu. Rev. Astron. Astrophys., 49, 471

Mundy, C. J., Curioni, A., Goldman, N., Kuo, I.-F., Reed, E., Fried, L. E., & Ianuzzi, M. 2008, J. Chem. Phys., 128, 184701

Nosé, S. 1984, Mol. Phys., 52, 255

Muñoz Caro, G. M., Meierhenrich, U. J., Schute, W. A., Barbier, B., Segovia, A. A., Rosenbauer, H., Thiemann, W. H.-P., Brack, A., & Greenberg, J. M. 2002, Nature, 416, 403

Oro, P. J. 1961, Nature, 190, 389

Plimpton, S. 1995, J. Comp. Phys., 117, 1, http://lammps.sandia.gov

Qi, T. & Reed, E. J. 2012, The Journal of Physical Chemistry A, 116, 10451

Raulin, F., Brasse, C., Poch, O., & Coll, P. 2012, Chem. Soc. Rev., 41, 5380

Reed, E. J. 2012, J. Phys. Chem. C, 116, 2205

Reed, E. J., Fried, L. E., & Joannopoulos, J. D. 2003, Phys. Rev. Lett., 90, 235503

Reed, E. J., Manaa, M. R., Fried, L. E., Glaesemann, K. R., & Joannopoulos, J. D. 2008, Nature Physics, 4, 72

Rendón, A., Carton, D. G., Sot, J., García-Pacios, M., Montes, L.-R., Valle, M., Arrondo, J.-L. R., Goñi, F. M., & Ruiz-Mirazo, K. 2012, Biophyscial Journal, 102, 278

Robertson, D. H., Brenner, D. W., & White, C. T. 1991, Phys. Rev. Lett., 67, 3132

Ross, D. S. 2006, J. Phys. Chem. A, 110, 6633

Sagan, C. & Khare, B. N. 1971, Science, 173, 417

Shoemaker, E. M. 1962, in The Physics and Astronomy of the Moon, ed. Z. Kopal (New York: Academic Press), 283–359

Snyder, L. E. & Buhl, D. 2012, Astrophys. J., 116, L42

Srinivasan, S. G., Goldman, N., Tamblyn, I., Hamel, S., & Gaus, M. 2014, J. Phys. Chem. A, 118, 5520

Zheng, G., Niklasson, A. M. N., & Karplus, M. 2011, J. Chem. Phys., 135, 044122

This manuscript was prepared with the AAS LaTeX macros v5.2.

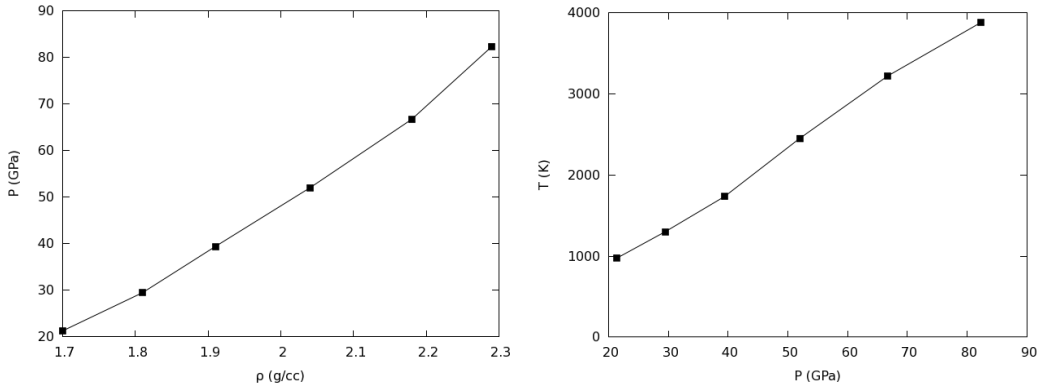

Fig. 1.— Hugoniot curves for shock compressed simulations achieved in the simulations.

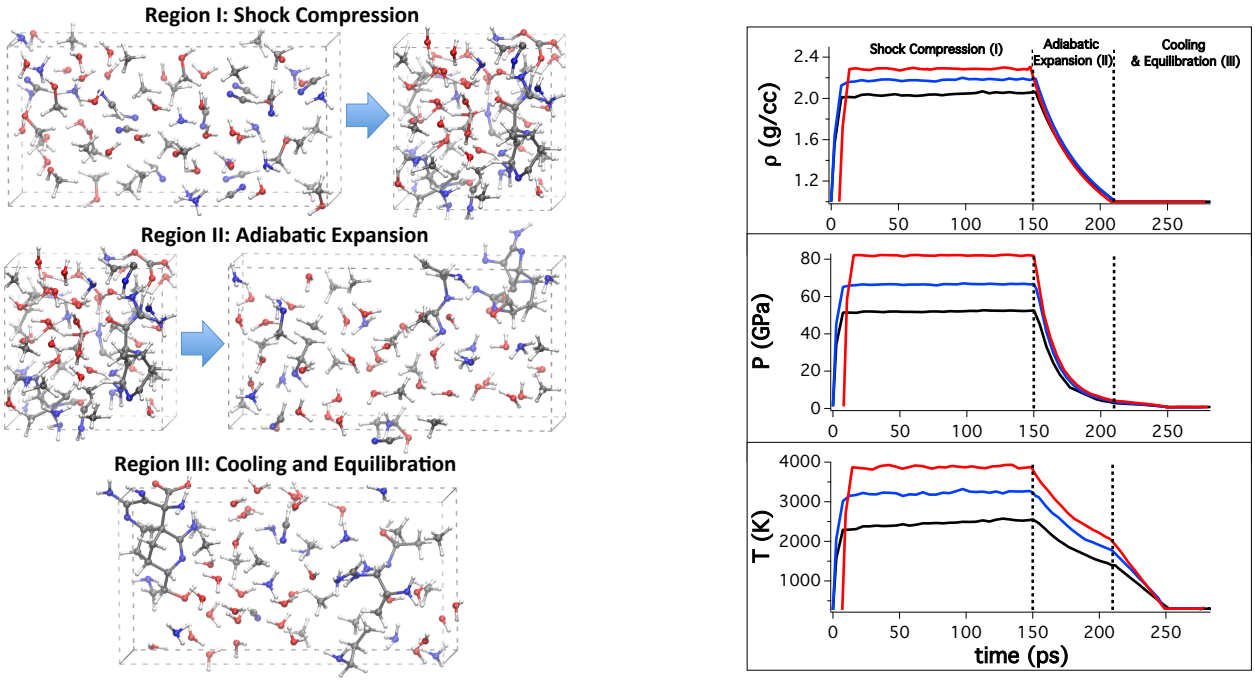

(a) (b)

Fig. 2.— Snapshots of simulations of (I) shock compression, (II) adiabatic expansion, and (III) cooling and equilibration, for peak thermodynamic conditions of 52 GPa and 2500 K (a), with traces of thermodynamic conditions explored during entire trajectories during for peak conditions exhibiting rapid chemical reactivity (b). Light blue circles correspond to carbon, dark blue to nitrogen, red to oxygen and white to hydrogen. In addition, the black line corresponds to peak conditions of 52 GPa, the blue line to 67 GPa, and the red line to 82 GPa. The thermodynamic conditions of the shock state vary depending on the impact velocity.

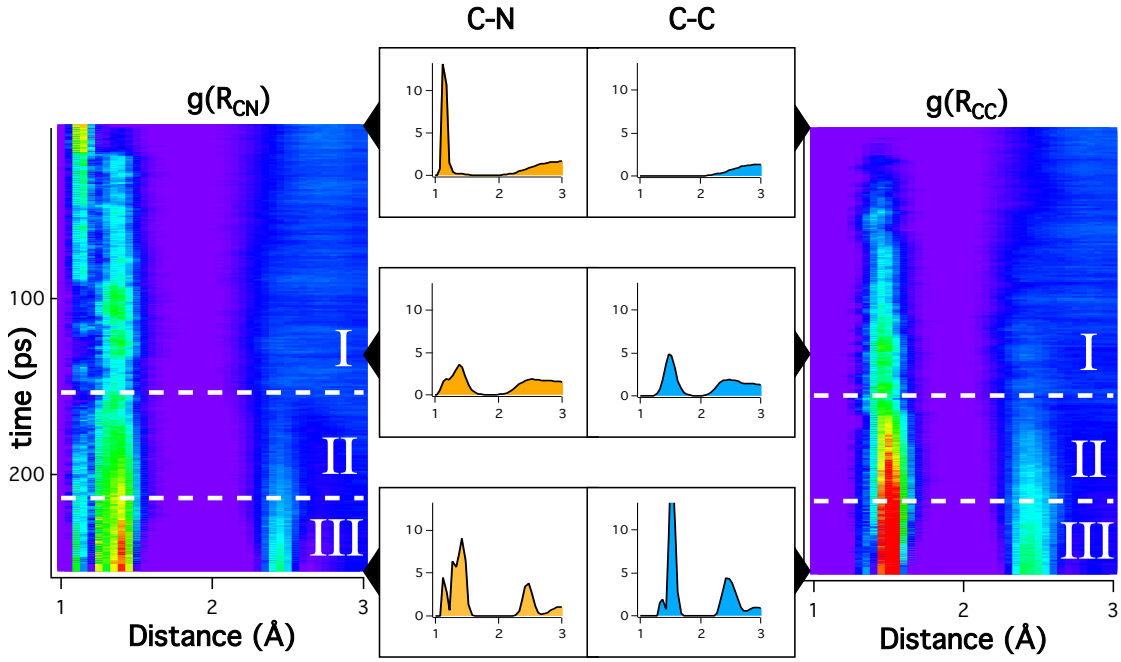

Fig. 3.— Time evolution of peak intensities of CC (left) and CN (right) RDFs at shock conditions of 52 GPa and 2500K. The middle panel shows profiles of the RDFs at different time points during the simulations during all three thermodynamic regions of our impact simulations.

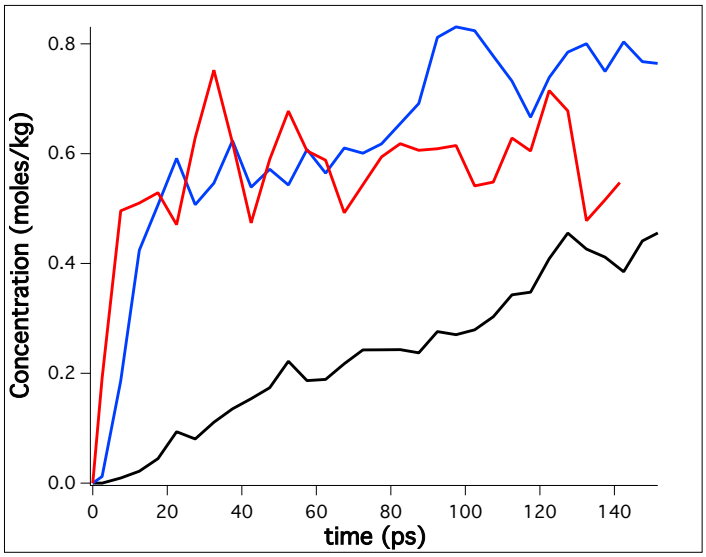

(a) C-C bond concentrations

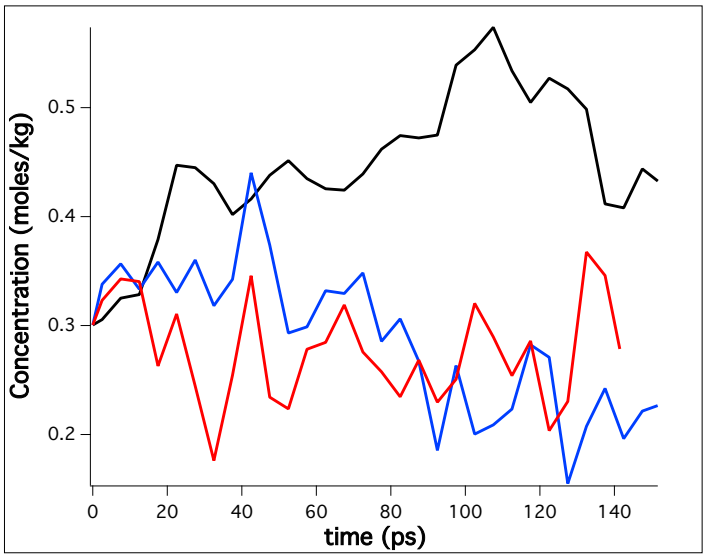

(b) C-N bond concentrations

Fig. 4.— Concentrations of CC, CN, and CO bonds during shock compression. Again, the black line corresponds to peak conditions of 52 GPa, the blue line to 67 GPa, and the red line to 82 GPa. Concentrations have been averaged over 0.5 ps intervals.

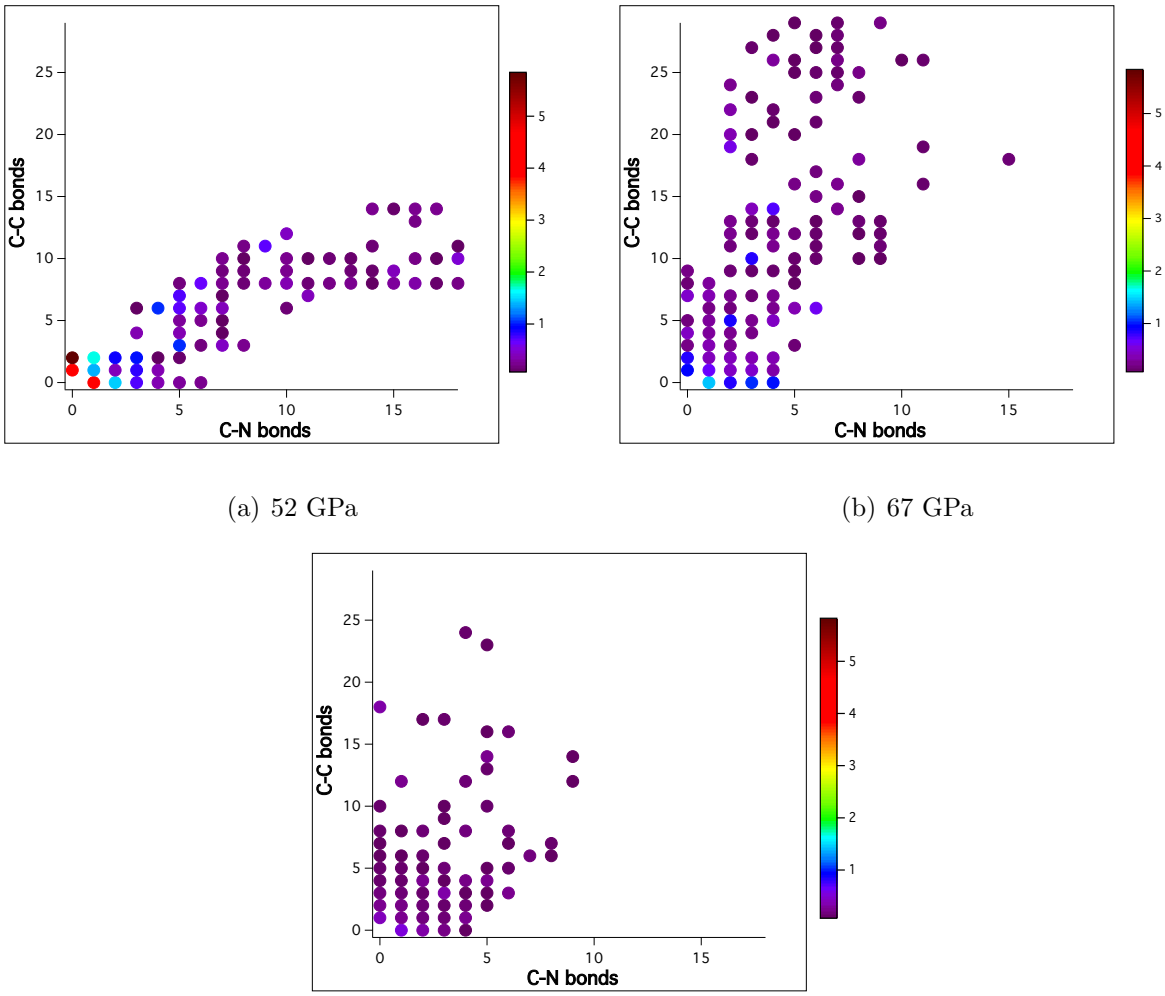

(a) 52 GPa

(b) 67 GPa

(c) 82 GPa

Fig. 5.— Average computed lifetimes of oligomeric CN-bonded species during shock compression. The colors correspond to mean lifetime of species with given ratio of CC/CN bonds. Shock compression to 52 GPa led to species with significant nitrogen content, while higher shock conditions led to predominantly carbon-containing species. Most species had lifetimes of less than 2 ps.

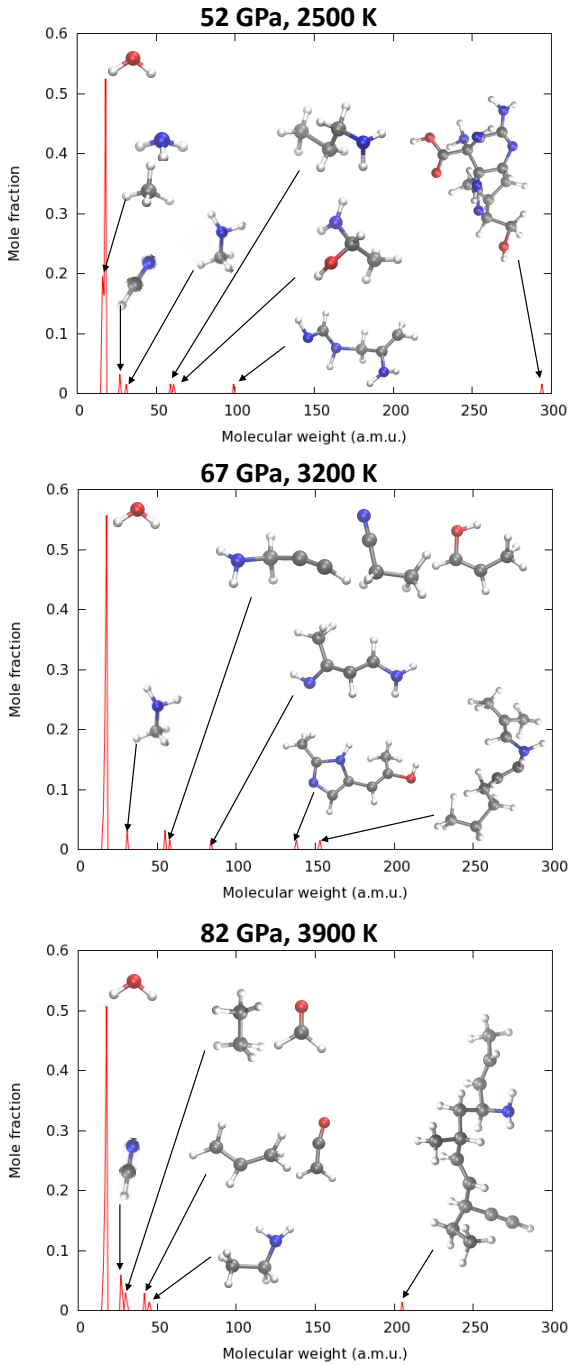

Fig. 6.— Simulated mass spectra for expansion products from different shock states, using the same previously mentioned color coding for each atom type.

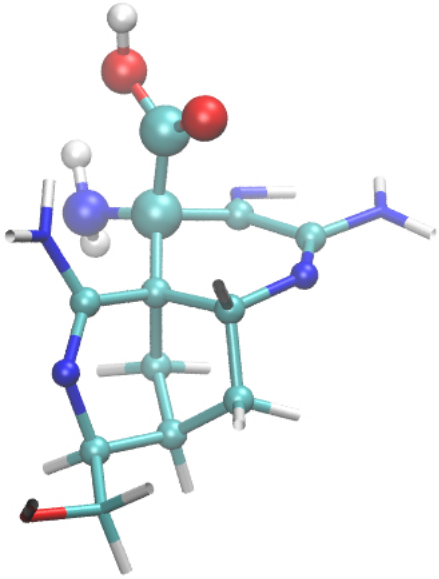

(a) Polycyclic aromatic hydrocarbon with glycine moiety (52 GPa)

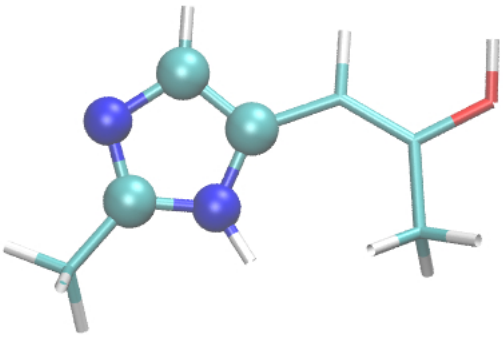

(b) Imidazole compound (67 GPa)

Fig. 7.— Aromatic compounds formed in our simulations, with peak shock pressures shown in parenthesis. For the amino acid in (a), the glycine moiety is highlighted with large spheres, and the aromatic rings with small spheres. The imidazole ring in (b) is highlighted in a similar fashion.